

Coupled Pairs of Quantum Rotors in $(\text{CH}_3)_2\text{SnCl}_2$: An Inelastic Neutron Scattering Study

M. Prager

Institut für Festkörperforschung, KFA-Jülich, Federal Republic of Germany

A. Heidemann

Institut Laue-Langevin, Grenoble, France

W. Häusler

Institut für Theoretische Physik der Universität Erlangen,
Federal Republic of Germany

Rotational tunnelling and librations of the methyl groups in $(\text{CH}_3)_2\text{SnCl}_2$ measured by inelastic neutron scattering are explained on the basis of coupled pairs of CH_3 groups. The self and the interaction part of the rotational potential are determined to be $(V_3, W_3) = (17.5 \text{ meV}, 10.9 \text{ meV})$. Thus, in agreement with our expectation from the crystallographic structure, the frustrated coupling is realized in $(\text{CH}_3)_2\text{SnCl}_2$ where the interaction W_3 counteracts the single particle potential V_3 .

Introduction

The dimethyl-tin-halides form an interesting class of substances among the intensively investigated organotin compounds [1]. In the dimethyl-tin-difluoride the tin atoms show an octahedral configuration [2]. The molecules are connected in a square plane network of Sn with bridging F and methyl groups pointing out perpendicularly of this plane. Thus the methyl groups themselves form a square plane of equally separated units. They are all equivalent. At $T_c = 66 \pm 5 \text{ K}$ the crystal shows a phase transition. The low temperature structure is not known but the methyl groups experience only a shallow rotational potential [3, 4] and are still equivalent [4]. It might be, that the low temperature phase differs from the high temperature structure only by the rotational ordering of the methyl groups.

The structure of dimethyl-tin-dichloride (DMTC) is related to the above one but distorted to a more tetrahedral configuration of the tin atoms [5] (Fig. 1): We still find layers of tin and chlorine atoms and of methyl groups, but the chlorine atoms are not localized on the straight line connecting two

Sn atoms, which are still arranged in a square lattice, and the bond axes of the methyl groups are now inclined to this plane. As a result of this structure the layer of methyl groups consists of pairs arranged side by side on inclined rotation axes and separated by $d_{cc} = 3.24 \text{ \AA}$. The closest distance between methyl groups of different pairs is $d'_{cc} = 4.61 \text{ \AA}$. On the basis of the structure we suggest pairwise coupled tunnelling methyl groups. Owing to a symmetry point just in between both methyl groups we additionally expect frustrated coupling [9]. The geometry is somewhat different to that in lithium acetate where both methyl groups of a pair are aligned on the same rotation axis [6], so a further contribution to the coupling term $\cos 3(\varphi_1 + \varphi_2)$ might play a role, which we did not take into account in this work.

Information related to the dynamics and the rotational potential of the methyl groups does not exist. The proton spin-lattice relaxation time is not measured so far. IR spectra were extended down to about 100 cm^{-1} only [1].

So far coupled quantum rotors were only observed in the limit of very shallow crystal potentials

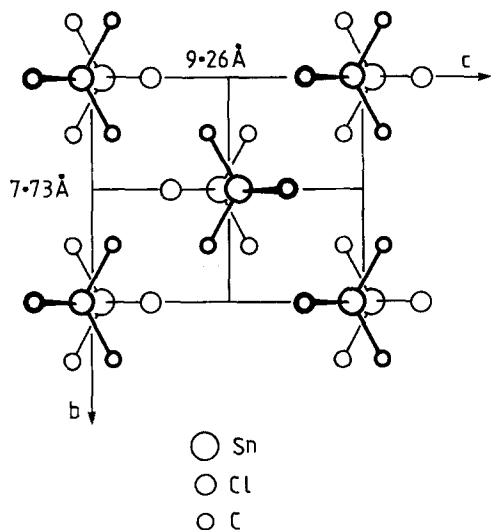


Fig. 1. Projection of the structure of $(\text{CH}_3)_2\text{SnCl}_2$ on the bc -plane according to Ref. 5. Large circles: Sn, medium circles: Cl, small circles: C of the CH_3 group. The distance of the two projected planes is $a/2=4.39 \text{ \AA}$

[6]. The present neutron scattering study wants to demonstrate the coupling of quantum rotors in a range of the rotational potential where the librational levels are already well defined but where the tunnelling splitting is still significant. In such a potential fewer levels are relevant at low temperatures and the theoretical description might be simpler. Such a weak rotational potential was expected by analogy to other methyl-tin-compounds [7, 8].

Experiments and Results

Commercially available DMTC powder was used in the experiments without further purification. The sample was mounted in a flat aluminium container in a standard He cryostat. The scattering probability was about 20%. Three different neutron spectrometers were used to cover the ranges of energy transfers $0.4 < \hbar\omega [\mu\text{eV}] < 200$ and $0.5 < \hbar\omega [\text{meV}] < 30$ with appropriate resolution. With the backscattering spectrometer IN 10 of the ILL, Grenoble, high resolution spectra were obtained with an energy resolution $\delta E = 0.4 \mu\text{eV}$ [FWHM] and for energy transfer $|\hbar\omega| \leq 5 \mu\text{eV}$. The thermal backscattering spectrometer IN 13 of the ILL has an energy resolution of $\delta E = 8 \mu\text{eV}$ [FWHM] and was used for the energy range up to $\hbar\omega = 200 \mu\text{eV}$. The regime of the lattice modes containing the methyl librations was investigated with the time of flight (TOF) spectrometer SV22 at the KFA Jülich. With various set-ups of this instrument the energy resolution was adjusted between $\delta E = (0.4 - 2.0) \text{ meV}$

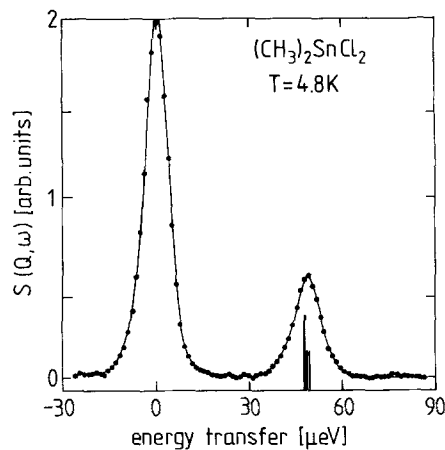


Fig. 2. Tunnelling spectrum of $(\text{CH}_3)_2\text{SnCl}_2$ as measured with the thermal backscattering spectrometer IN13 of the ILL, Grenoble, with an energy resolution $\delta E_0 = 8 \mu\text{eV}$ [FWHM]. The solid line represents a fit with 3 Gaussians of finite and equal intrinsic width (see the text). The bars represent the positions and intensities of tunnelling transitions in the model of two coupled methyl groups

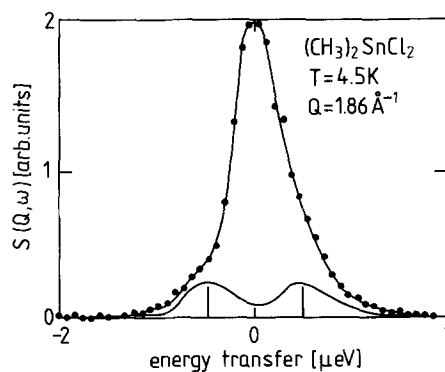


Fig. 3. Tunnelling spectrum of $(\text{CH}_3)_2\text{SnCl}_2$ in the very high resolution range, measured with the backscattering spectrometer IN10 of the ILL, Grenoble, using an energy resolution $\delta E_0 = 0.4 \mu\text{eV}$ [FWHM]. The solid line is a fit with a resolution function and two broadened inelastic lines. The bar represents a tunnelling transition as calculated in the model of two coupled methyl groups

covering thus the range of energy transfers up to $\hbar\omega < 30 \text{ meV}$.

The measured spectra were converted into $S(Q, \omega)$. Figure 2 shows the spectrum measured with IN13. A well defined transition is found at $\hbar\omega_{\text{tun}} = 49 \mu\text{eV}$. The line is somewhat broader than the instrumental resolution. A fit with a Gaussian line reveals an intrinsic width $\Gamma_{\text{tun}} = 2.8 \pm 0.2 \mu\text{eV}$ [HWHM]. In the very high resolution spectrum from IN10 (Fig. 3) we observe an inelastic feature close to the elastic line. If we fit the spectrum with a resolution function plus two inelastic lines symmetric to it we obtain $\hbar\omega_{\text{tun}} = 0.7 \mu\text{eV}$. This result is strongly dependent on the assumptions on the intensity and

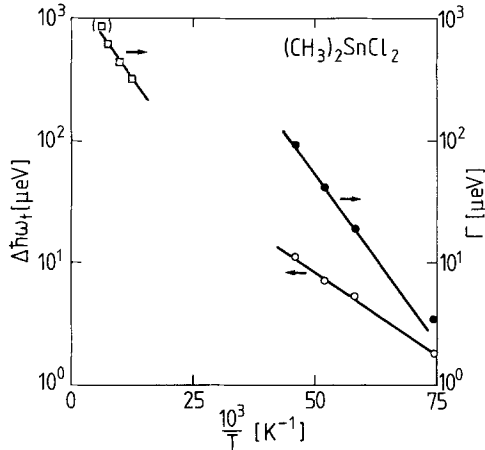


Fig. 4. Arrhenius plot of the shift $\Delta\hbar\omega_t$ and broadening Γ_t of the tunnelling transition at $\hbar\omega=49 \mu\text{eV}$. Activation energies $E_a^s=5.4 \text{ meV}$ and $E_a^r=9.2 \text{ meV}$ are derived. The high temperature values belong to classical reorientation and are extracted from Fig. 5 and similar spectra

line width of the inelastic lines as further discussed below. The tunnelling line at $\hbar\omega_{\text{tun}}=49 \mu\text{eV}$ shifts to lower energies and broadens with increasing temperature. Assuming a Lorentzian broadening, the shift and the width obey Arrhenius laws (Fig. 4) with different activation energies $E_a^s=(5.4 \pm 0.2 \text{ meV})$ and $E_a^r=9.2 \pm 2 \text{ meV}$ and corresponding prefactors $\hbar\omega_{0t}=0.2 \text{ meV}$ and $\Gamma_{0t}=30 \text{ meV}$. The large error bar of E_a^r is a consequence of the intrinsic structure of the tunnelling line.

Some quasielastic spectra which are a consequence of classical reorientation of the methyl groups were measured at elevated sample temperatures ($T > 80 \text{ K}$) with an energy resolution $\delta E=0.4 \text{ meV}$ using $\lambda_0=4.0 \text{ \AA}$ at the TOF spectrometer SV 22. One representative spectrum is shown in Fig. 5. The quasielastic scattering is rather well described by a single Lorentzian. We find the same activation energy for the classical reorientation as for the broadening of the tunnelling transition (in Fig. 4) but the prefactors is considerably smaller $\Gamma_{00}=1.6 \text{ meV}$.

An overview of the excitations in the meV regime was obtained with the same spectrometer with an incident energy $E_0=35 \text{ meV}$ and a resolution $\delta E_0=1.9 \text{ meV}$. In the spectrum shown in Fig. 6 all detectors in the angular range $30^\circ < 2\theta \leq 130^\circ$ have been added to give good statistics. The dominant feature of the spectrum is a peak at an energy transfer $E=5.5 \text{ meV}$. The peak has an intrinsic width of about 1 meV . At higher energies there are additional peaks in the density of states: A broad component at about $11 \pm 2 \text{ meV}$, a weak peak at 15 meV and an asymmetric peak between 19 and 23 meV . The three peaks with energies below 15 meV are strongly

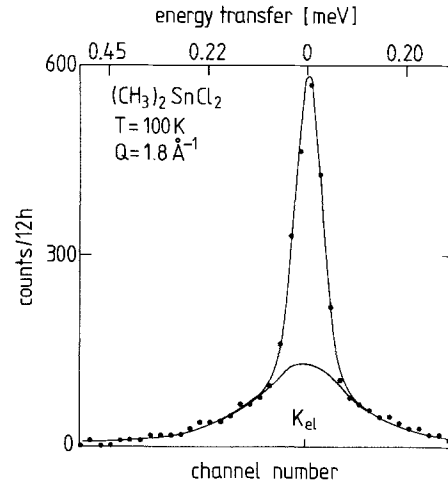


Fig. 5. Quasielastic scattering of $(\text{CH}_3)_2\text{SnCl}_2$ at $T=100 \text{ K}$ as measured with the thermal time of flight spectrometer SV 22 of the KFA, Jülich, using an energy resolution $\delta E_0=0.40 \text{ meV}$. The solid line is a fit with a Gaussian representing the elastic line and a Lorentzian line. The spectrum is shown as counts vs. time. The nonlinear energy scale is shown on the top

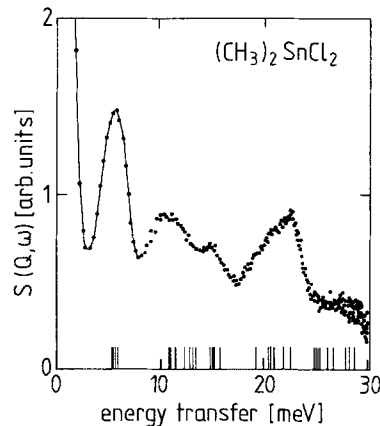


Fig. 6. Excitations in the lattice regime of $(\text{CH}_3)_2\text{SnCl}_2$ as measured with the TOF spectrometer SV 22 of the KFA Jülich with an elastic energy resolution of $\delta E_0=1.9 \text{ meV}$. The measured spectrum is converted into $S(Q, \omega)$. The solid line is a guide to the eye only. The bars represent calculated transition energies (see the text)

damped with increasing temperature while the spectrum is little changed around 21 meV . The prominent peak at 5.5 meV is strongly damped with increasing temperature. It was investigated with the improved resolution $\delta E_0=0.65 \text{ meV}$ using neutrons of $\lambda_0=2 \text{ \AA}$ with the 3rd order Bragg reflection of the pyrolytic graphite-monochromator crystals. Spectra obtained at three different temperatures are shown in Fig. 7. For intensity reasons all detectors are summed up. The peak is now clearly split into a doublet. The line positions are $E_1=4.4 \text{ meV}$ and $E_2=5.8 \text{ meV}$ at $T=15 \text{ K}$. These positions nearly do

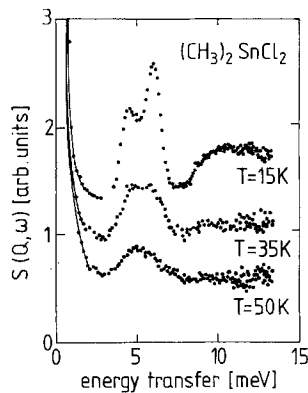


Fig. 7. High resolution spectra of the peak at ~ 5.8 meV of $(\text{CH}_3)_2\text{SnCl}_2$ as measured with the TOF spectrometer SV 22 with an elastic energy resolution $\delta E_0 = 0.65$ meV for the three indicated sample temperatures

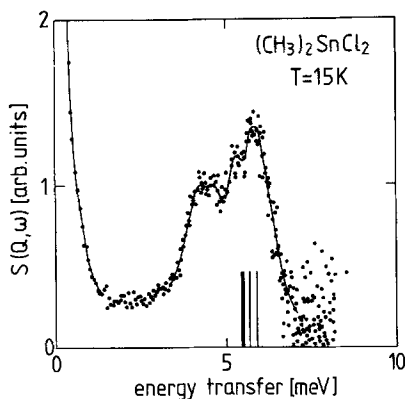


Fig. 8. The same peak as shown in Fig. 7 measured with an even improved energy resolution $\delta E_0 = 0.4$ meV with the TOF spectrometer SV 22. The solid line is a guide to the eye only. The bars represent transition energies calculated in the model of pairs of coupled methyl groups

not shift with temperature but the intensities of both peaks strongly decrease with the sharper peak at $E_2 = 5.8$ meV disappearing faster. With improved resolution $\delta E_0 = 0.4$ meV we find (Fig. 8) that the peaks of the doublet again have an internal structure of a shape suggested by the solid line. The spectrum was measured for 90 h and thus we now have reached the limit of our spectrometer.

Discussion

Based on the crystal structure we interpret our data as a result of rotational tunnelling of pairs of coupled methyl groups. The strongest experimental evidence for this is contained in the tunnelling spectrum showing a weak line at ~ 1 μeV and a strong and broad one at 49 μeV . The weak tunnelling line

can hardly be assigned to a weak component of inequivalent methyl groups as there is no evidence for such a component in the structure. It is however a natural consequence of a coupling of pairs of methyl groups. Similar spectra were found for lithium acetate [6]. Quantum mechanical models for coupled tunnelling rotors [6, 9] were calculated for the Hamiltonian

$$H(\varphi_1, \varphi_2) = -B \frac{\partial^2}{\partial \varphi_1^2} - B \frac{\partial^2}{\partial \varphi_2^2} + V(\varphi_1) + V(\varphi_2) + W(\varphi_1, \varphi_2). \quad (1)$$

Here $B = \hbar^2/2\theta = 647.5$ μeV is the rotational constant of the methyl groups. The single particle potentials are described by the first term of a Fourier expansion

$$V(\varphi_i) = V_3 \cdot \cos 3\varphi_i, \quad (2)$$

and as the simplest interaction, which is $\frac{2\pi}{3}$ periodic in φ_i

$$W(\varphi_1, \varphi_2) = W_3 \cdot \cos \{3(\varphi_1 - \varphi_2)\}. \quad (3)$$

The Hamiltonian (1), with (2) and (3), is the simplest assumption for two coupled methyl groups aligned on the same rotation axis [9]. It has been shown in a rigorous treatment of two coupled inclined methyl groups [10, 11] that it also represents the simplest nontrivial model for this geometry. No quantitative agreement with the experimental data can be expected from such a model, but it should reproduce the general features. Using the Hamiltonian (1) the tunnelling transition at 49 μeV must be a triplet which is supported by the finite width of this peak found in the experiment. Unfortunately the suggested internal structure cannot be resolved with any available spectrometer, but it can be related to the low energy transition observed with IN10, as can be seen from the level scheme (insert in Fig. 9). The figures on each transition line indicate the multiplicity of this transition. No transition matrix elements are calculated so far for coupled rotors, but the smallness of $\hbar\omega_3/\hbar\omega_0$ indicates, that intensities should be well approximated by using Hartree wave functions for each single rotor. This leads to intensity relations between the four tunnelling lines simply determined by spin multiplicities. Thus we performed a common fit of the two spectra with a pattern of 4 lines of relative intensities 1:4:2:2. Every single line has been provided with a common width, which might result from interpair coupling. The line shape was approximated by a Gaussian $\exp(-x^2/\Gamma_t^2)$.

Thus since our tunnelling lines are not well resolved the results of a combined fit of the two tun-

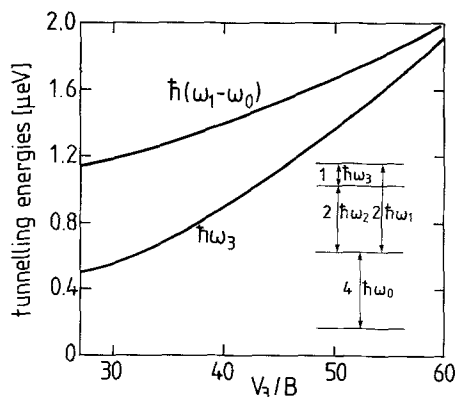


Fig. 9. Tunnelling transition energies of a coupled pair of methyl groups along a path in the parameter space (V_3, W_3) which keeps $\hbar\bar{\omega}_i = \text{const} = 49 \mu\text{eV}$. The level scheme is shown as insert. The numbers give the multiplicities of the corresponding transition. $\hbar(\omega_1 - \omega_0)$ is a measure of the width of the transition line at energy $\hbar\bar{\omega}_i$. $\hbar\omega_3$ corresponds to the weak transition at the lowest energy

nelling spectra depend strongly on the assumptions which enter in the data analysis as e.g. the line intensities, whether the elastic line is contaminated or not, etc. While the average position $\hbar\bar{\omega}_i = \frac{1}{4}(2\hbar\omega_0 + \hbar\omega_1 + \hbar\omega_2) = 49 \mu\text{eV}$ is well established the shallow line is compatible with splittings $\hbar\omega_3 = 0.5 \div 1.5 \mu\text{eV}$ because of a strong correlation between line position, line width Γ_i and line intensity.

The most consistent description could be obtained for $\Gamma_i = 2.6 \mu\text{eV}$ and transition energies $\hbar\omega = 0.6, 48.4, 49.0, 49.6 \mu\text{eV}$, but for other values of Γ_i and resulting different $\hbar\omega_i$ (especially $\hbar\omega_3$) the fits also were not bad. Thus it was difficult to extract the two parameters V_3, W_3 of the potential from the tunnelling transitions alone and it was very important to have the energy of the first excited librational state as a further experimental information.

The experiment presented in Fig. 6 seems to give a clear information on the methyl libration but it required an extensive careful study to get a convincing answer. In most materials containing methyl groups the methyl libration is the motion with the largest hydrogen amplitude $\langle u^2 \rangle$ because of the shallowness and anharmonicity of the rotational potential. Thus it produces the strongest incoherent neutron scattering peak. The dominant peak, however, is a doublet (Fig. 7). This structure could be caused by a dispersion of the librational mode due to coupling. The different temperature dependence of the two sublimes showed, however, that the two parts of the line must be of different origin. Because of the much stronger damping with temperature we interpret the high energy part at $E_{01} = 5.8 \text{ meV}$ as libration, which finally in the very high resolution experiment (Fig. 8) is found to have again - now a

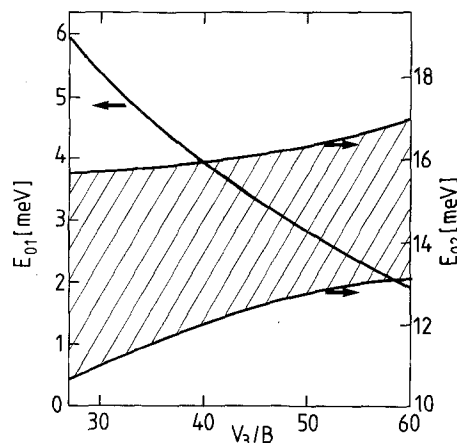


Fig. 10. Librational energies of a coupled pair of methyl groups for the same conditions as Fig. 9. Shaded area: energy band consisting of 12 transitions to the second and higher excited librational levels, altogether called E_{02}

much narrower - fine structure: The splitting is $\Delta \approx 0.2 \text{ meV}$ only.

The most obvious information about the system of coupled rotors is still the overall tunnelling splitting $\hbar\bar{\omega}$. Thus we calculate in the parameter space (V_3, W_3) the eigenvalues of the coupled rotors along a path $\hbar\bar{\omega} = 49 \mu\text{eV}$. This is shown for the tunnelling transitions in Fig. 9 and for the librational transitions in Fig. 10. In both figures V_3 is chosen to parametrize this path. We can now use our well defined first excited librational energy to get the most appropriate set of potential parameters. Using

$$(V_3, W_3) = (17.5 \text{ meV}, 10.9 \text{ meV})$$

it is possible to reproduce all observed transition energies extremely well. We obtain tunnelling transition energies $\hbar\omega_i = 0.47, 48.15, 48.77$ and $49.24 \mu\text{eV}$ and librational energies $E_{01} = 5.46, 5.47, 5.66$ and 5.89 meV . The calculated values are shown as bars in the measured spectra (Figs. 2, 3, 8). The width of the tunnelling line at $40 \mu\text{eV}$ ($\hbar(\omega_1 - \omega_0)$) and the weak line at $0.5 \mu\text{eV}$ ($\hbar\omega_3$) are in as good agreement with the measured data as is the overall splitting (0.3 meV) of the first excited librational state. It is worth to report that an attempt to fit the observed tunnelling spectrum with a coupling term $W_3 < 0$ (i.e. not frustrated coupling) led to librational energies greater than 7 meV . So our guess on the type of coupling on the basis of crystallography is confirmed by the model. It even reproduces the next transition, which is observed in the range $9 \div 13 \text{ meV}$, rather well: we calculate an excitation band consisting of 12 lines in the energy range $10.7 \div 15.7 \text{ meV}$. The calculated transition energies are shown as bars in Fig. 6. A

more quantitative comparison of calculated and observed spectra would require the transition intensities, which are different for different symmetry species and also dependent on Q . The latter varies in a time of flight spectrum with the energy transfer.

The shift and broadening of the tunnelling lines with temperature is due to the coupling of the pair of tunnelling rotors to the phonons of the crystal. For isolated methyl groups a theoretical description has been given by Hewson [12]. In the strong oscillator limit only the two lowest librational levels have to be taken into account and the theory predicts a broadening of the lines according to an Arrhenius law with an activation energy E_{01} and a shift with $E_a < E_{01}$. These predictions are confirmed for many rather strongly hindered tunnelling rotors. In DMTC, however, we have found $E_a^S = 5.4$ meV $\sim E_{01}$ and $E_a = 9.2$ meV $> E_{01}$ in contradiction to [12]. Two reasons can be suggested for this discrepancy: *i*) In DMTC the methyl groups rotate in a rather shallow potential and the temperature dependence of rotational tunnelling cannot be described in the strong oscillator limit. More levels would have to be included in the calculations. *ii*) Due to the coupling the librational levels split and the sequence of excitations becomes rather dense and complex (see the calculated levels in Fig. 6). Thus it is not astonishing that in DMTC our observations are not in agreement with the classical theory. A recent work [13] extends the theory [12] to systems of coupled pairs of methyl groups by using the more complex librational level scheme of such a system, but still discusses the temperature dependence in the strong oscillator limit by including only the lowest two librational levels (now split by coupling). Our model shows, that in DMTC the librational levels E_{01} and E_{02} overlap, and thus the restriction to a split E_{01} state cannot be sufficient for a correct description of the temperature dependence of tunnelling. The theory shows however already, that activation energies E_a different from E_{01} are possible.

There is still the question about the meaning of the second strong low energy peak at $E \sim 4.4$ meV. We suggest that it could be caused by a clockwise – anticlockwise rotation of the molecules around the c -axis and coupled along the b axis via their methyl groups (cf. Fig. 1). Experiments with the deuterated compound could confirm the assumption that this peak is not produced by CH_3 -rotation.

Conclusion

We have measured the tunnelling splitting of the librational groundstate of the methyl groups in

$(\text{CH}_3)_2\text{SnCl}_2$ and their temperature dependence. The corresponding librational energies are extracted from temperature dependent high resolution measurements of the density of states. Both, tunnelling and librational energies can be very well described in a model of coupled pairs of methyl groups. The coupling term in the potential counteracts the single particle term (frustrated coupling), in agreement with the crystallographic structure. The temperature dependence of the tunnelling splitting cannot be described adequately in the strong oscillator limit for which theories have been developed so far. Further theoretical work is desirable.

References

1. Gmelin Handbook of Inorganic Chemistry. 8th Ed., Vols. 1–12. Berlin, Heidelberg, New York, Tokio: Springer 1984
2. Schlemper, E.O., Hamilton, W.C.: Inorg. Chem. **5**, 995 (1966)
3. Steenbergen, Chr., Rush, J.J.: J. Chem. Phys. **70**, 50 (1979)
4. Alefeld, B., Heidemann, A., Prager, M.: (to be published)
5. Davies, A.G., Milledge, H.J., Puxley, D.C., Smith, P.J.: J. Chem. Soc. (A) 2862 (1970)
6. Clough, S., Heidemann, A., Horsewill, A.H., Paley, M.N.J.: Z. Phys. B – Condensed Matter **55**, 1 (1984)
7. Prager, M., Müller-Warmuth, W., Duprée, K.H.: Z. Phys. B – Condensed Matter **51**, 309 (1983)
8. Prager, M., Weiss, A., Da Zhang: (to be published)
9. Häusler, W., Müller, A.: Z. Phys. B – Condensed Matter **59**, 177 (1985)
10. Swalen, J.D., Costain, C.C.: J. Chem. Phys. **31**, 1562 (1959)
11. Grant, D.M., Pugmire, R.J., Livingston, R.C., Strong, K.A., McMurphy, H.L., Brugger, R.M.: J. Chem. Phys. **52**, 4424 (1970)
12. Hewson, A.C.: J. Phys. C **15**, 3841 and 3855 (1982)
13. Huggins, J.G.: Z. Phys. B – Condensed Matter **59**, 293 (1985)

M. Prager
Institut für Festkörperforschung
Kernforschungsanlage Jülich GmbH
Postfach 1913
D-5170 Jülich 1
Federal Republic of Germany

A. Heidemann
Institut Max von Laue-Paul Langevin
156 X
F-38042 Grenoble Cedex
France

W. Häusler
Universität Erlangen
Glückstrasse 6
D-8520 Erlangen
Federal Republic of Germany